Bioorganic & Medicinal Chemistry 18 (2010) 2255–2264

Contents lists available at ScienceDirect

Bioorganic & Medicinal Chemistry

journal homepage: www.elsevier.com/locate/bmc

Synthesis, radiofluorination, and hypoxia-selective studies of FRAZ: A configurational and positional analogue of the clinical hypoxia marker, [^{18}F]-FAZA

Piyush Kumar *, Ebrahim Naimi, Alexander J. McEwan, Leonard I. Wiebe

Division of Oncologic Imaging, Department of Oncology, University of Alberta, Cross Cancer Institute, 11560 University Ave., Edmonton, Canada T6G1Z2

ARTICLE INFO

Article history:
Received 18 November 2009
Revised 20 January 2010
Accepted 22 January 2010
Available online 6 February 2010

Keywords:
Tumor hypoxia
FRAZ
Azomycin nucleoside-based radiosensitizer
Positron emission tomography (PET)

ABSTRACT

The current work evaluates 1-α-D-(2-deoxy-2-fluororibofuranosyl)-2-nitroimidazole (FRAZ), a novel azomycin nucleoside that is a potential radiosensitizer of tumor hypoxia. FRAZ is a ribose analogue of 1-α-D-(2-deoxy-2-fluoroarabinofuranosyl)-2-nitroimidazole ([^{18}F]-FAZA), a clinically used hypoxia marker. Preliminary assessment of the cytotoxicity and hypoxia-specific in vitro binding in HCT-110 colorectal cancer cells indicate that the radiosensitization properties of FRAZ are similar to that of FAZA, with a sensitizer enhancement ratio (SER) of ~1.8. An automated radiosynthesis of [^{18}F]-FRAZ using a commercial automated synthesis unit (ASU) was established (synthesis time ~32 min; radiochemical yield (decay uncorrecetd) ~22%) to facilitate its application in PET-based diagnosis of hypoxic tumors.

1. Introduction

Hypoxic cells are viable, oxygen deficient, cells that are generally 2.5 to 3-fold more radioresistant than well-oxygenated cells to the cytotoxic effects of ionizing radiation (oxygen effect). Hypoxia develops in many solid tumors, leading to the induction of adaptive genomic transcriptional and post-translational changes[1–4] that promote the establishment of an aggressive phenotype which induces metastatic potential, promotes angiogenesis and supports local disease progression.[5–8] Inadequate angiogenesis and compression of blood and lymphatic vessels in rapidly proliferating tumor cells change the composition and structure of the extracellular matrix (ECM), which effectively reduces perfusion of the tumor[9] and, consequently, decreases the delivery of the drugs to the hypoxic area. Since hypoxic tumor cells have an aggressive and treatment-resistant phenotype, they respond poorly to radiotherapy (external beam radiotherapy; XRT) and are major determinants of XRT failure.[10] This necessitates early identification of hypoxic tumor cells[11,12] and aggressive, innovative treatment to combat their rapid progression and the resultant poor prognosis.[8,13]

2-Nitroimidazoles (azomycins) have proven radiosensitization and chemosensitization properties in viable but hypoxic cells[14] (Nagasawa et al., 2006), restoring the 'oxygen effect' (i.e., normalizing radiosensitivity) through an oxygen-mimicking process (radiosensitizer effect) that results from their selective bio-reductive activation and consequent adduct formation to hypoxic tissue components.[15,16] The first-electron reduction ($^1E_7$) step is crucial, and is reversible in the presence of oxygen. Therefore, the selectivity and the degree of binding of a radiosensitizer is a function of its electron affinity and the concentration of oxygen in cells. Reducing equivalents (electrons) are metabolically derived,[17] and therefore the adduct-based accumulation of azomycins is restricted to viable but oxygen-deficient tissues, with no accumulation in necrotic cells, and little accumulation and low toxicity in most normally-oxygenated cells. If the single-electron reduction potential at pH 7 ($^1E_7$) approaches that of O_2 (−155 mV), then selectivity for hypoxia will be diminished; if the drug is not sufficiently electron-affinic ($^1E_7$ <−450 mV), then sensitivity will be lost. The $^1E_7$'s of most 2-nitroimidazoles, for example, misonidazole (MISO), lie around −390 mV, the region for optimal selectivity[18] and sensitivity.[19,15,20] Nitroimidazole-based radiosensitizers, when radiohalogenated[11,12,21,22] with radioiodine or radiofluorine, are of interest as radiodiagnostics for imaging focal hypoxia, providing in vivo pre- and post-therapeutic evaluation of cancer patients.[12] Hypoxia imaging is also of interest in determining the role of hypoxia-upregulated transcription factors such as hypoxia-inducible factor-1α (HIF1α)[23] and glucose transporter proteins (GLUTs)[24] to the therapeutic sensitivity of hypoxic tissues at cellular and molecular levels,[16,25] for PET mapping of heterogeneity in hypoxic tissues,[24] and to obtain valuable information on therapeutic efficacy and the development of new treatment modalities.

* Corresponding author. Tel.: +1 780 989 4313; fax: +1 780 432 8483.
E-mail addresses: pkumar@ualberta.ca (P. Kumar), ebinaimi@hotmail.com (E. Naimi).

0968-0896/$ - see front matter © 2010 Elsevier Ltd. All rights reserved.
doi:10.1016/j.bmc.2010.01.064

Hypoxic cancer cells can bio-reductively activate radiosensitizers via reductive enzymes that are upregulated in hypoxia.[26] Properties of hypoxia-selective radiosensitizers that will maximize their accumulation in hypoxic cells include minimal in vivo metabolism other than reductive bio-activation, short residence time in non-target tissues, rapid renal excretion and low hepatobiliary clearance. 2-Nitroimidazole-based molecules enter cells ubiquitously via diffusion, and are selectively trapped by bio-reductive activation in hypoxic cells. This means that increasing the lipophilicity of a radiosensitizer[27] will increase its non-specific accumulation in lipoidal tissues and contribute to selective toxicities (e.g., neuropathies), whereas lowering lipophilicity will increase renal clearance and reduce accumulation in the liver. ^{18}F-labeled 1-(2-nitroimidazole)-3-fluoro-2-propanol ([^{18}F]-fluoromisonidazole, [^{18}F]-FMISO) was one of the first 2-nitroimidazole-based tracers used in positron emission tomography (PET) to diagnose oncological hypoxia (Fig. 1). It is currently an important clinical tool in diagnostic oncology.[28] Extensive pharmacokinetic (PK) and hypoxia-selective uptake studies have been used to validate this tracer.[21,22,29,30] However, its major disadvantage lies in its relatively slow clearance from normal tissues.[31] Other nitroimidazole-based PET tracers that have found limited clinical utility include EFI[32] and FETNIM.[33]

The optimal hypoxia-selective reductive binding potential and faster clearance properties of several radioiodinated sugar-coupled 2-nitroimidazoles (e.g., 1-α-D-(5-deoxy-5-iodoarabinofuranosyl)-2-nitroimidazole ([^{123}I]-IAZA), in comparison to non-sugared azomycins, led to their clinical advancement as imaging radiodiagnostics using single-photon-emission computed tomography (SPECT).[34–36] Exploitation of the shorter half-life of F-18 (~110 min compared to 13 h for I-123) and the superior image resolution of PET formed the basis to develop ^{18}F-labeled 1-α-D-(5-deoxy-5-fluoroarabinofuranosyl)-2-nitroimidazole ([^{18}F]-FAZA).[37–41] In a recent study, the in vitro cell uptake and in vivo imaging parameters of [^{18}F]-FAZA were compared with those of the established tracer [^{18}F]-FMISO.[42,43] The advantage of [^{18}F]-FAZA appears to lie in its faster clearance from the body, resulting in shorter waiting times after tracer application and perhaps a lower radiation exposure.[42,44] [^{18}F]-FAZA is currently being used in several tumor hypoxia based clinical diagnostic studies.[12,45,46] Radiodosimetric calculations with [$^{123/131}$I]-IAZA, a radioiodinated azomycin nucleoside, indicate possible use of these compounds in molecular radiotherapy (MRT).[34] Surprisingly, evaluations of these azomycin halonucleosides as radiosensitizers for therapeutic XRT have not been reported.

Radiolabeled FAZA and IAZA, radiodiagnostics used extensively in the nuclear medicine community, are C-5′ substituted azomycin nucleosides; they have free hydroxyl groups at C-2′ and C-3′, and a strongly electron-withdrawing nitro group at the C-5 imidazole position which may consequently become involved in secondary intramolecular reactions with neighboring nucleophilic substituents (Fig. 1, structure of the C-2′-C-5 cyclic product). The latter reaction competes with fluorination of the precursor during the radiolabeling process, resulting in poor fluorination yields.[47] In addition, the fluorine atom in FAZA is located at C-5′; as a primary alkyl fluoride it is also prone to in vivo hydrolysis (Fig. 1). Certainly, deiodination of [^{123}I]-IAZA, the corresponding iodinated analogue, occurs in vivo.[48] It is postulated that placement of fluorine on a secondary carbon, that is, C-2′, as in FRAZ, may provide additional chemical stability to the molecule[49,50] thereby offering fewer side products during the synthesis of FRAZ (and the corresponding [^{18}F]-labeled radiopharmaceutical) while still maintaining the clinically desirable properties (e.g., optimal lipophilicity and hypoxia-selective reductive activation) of FAZA. The current work describes the synthesis of 1-α-D-(2-deoxy-2-fluororibofuranosyl)-2-nitroimidazole (FRAZ, **7**), the automated F-18 radiolabeling to manufacture [^{18}F]-FRAZ ([^{18}F]-**7**), its preliminary hypoxia-selective radiosensitization potency in the HCT-110 colorectal cancer cells in vitro, and assessment of its in vitro cytotoxicity using a bank of cancer cell lines.

2. Results and discussion

2.1. Chemistry

The syntheses of **7** and [^{18}F]-**7** were derived from 1-α-D-(3,5-di-*O*-benzoylarabinofuranosyl)-2-nitroimidazole, **2**. This molecule features a 2′-OH group for reaction with DAST to afford **6** (Scheme 1), or for elaboration with an appropriate leaving group, for example, trifluoromethanesulfonyl (triflate), 4-nitrobenzenesulfonyl (nosylate), or toluenesulfonyl (tosylate), to afford the precursors, **11a–11c**, for making [^{18}F]-**7** (Scheme 2). Thus, the treatment of 1-α-D-(arabinofuranosyl)-2-nitroimidazole (AZA, **8**)[51] with benzoyl chloride in anhydrous pyridine afforded **1** in quantitative yield (100%; Scheme 1). Selective 2′-O-debenzoylation of **1** was attempted following a literature method,[52] however in our case, treatment of **1** with potassium *tert*-butoxide (*tert*-BuOK; 3 equiv) in tetrahydrofuran (THF) at −56 °C for 5 min gave 1-α-D-(3-*O*-benzoylarabinofuranosyl)-2-nitroimidazole, **4**, a mono benzoylated derivative as a major product (42% yield). ^{1}H NMR spectroscopy confirmed the formation of this compound by demonstrating two doublet (d) signals for H-2′ and H-3′ at δ 4.31 and 4.05 ppm, respectively, that moved upfield in comparison to corresponding resonances in **1**. In addition, this reaction also afforded 1-α-D-(3,5-di-*O*-benzoylarabinofuranosyl)-2-nitroimidazole, **2**, 1-α-D-(2,5-di-*O*-benzoylarabinofuranosyl)-2-nitroimidazole, **3**, and a 5′-O-monobenzoylated analogue, 1-α-D-(5-*O*-benzoylarabinofuranosyl)-2-nitroimidazole, **5**, albeit in smaller quantities (totaling ~40%). It was observed that **1**, when reacted with an equimolar quantity of *tert*-BuOK in THF (1 equiv) at a relatively low temperature (−78 °C), afforded the 2′-debenzoylated product, **2**, in excellent yield (~81%) in 30 min (Scheme 1). A strong upfield movement of the chemical shifts of H-2′ (by δ 1.21 ppm) and C-2′ (by δ 7.02 ppm) in the ^{1}H NMR spectrum of **2** in comparison to the tribenzoylated product **1** confirmed this selective debenzoylation at C-2′-OH.

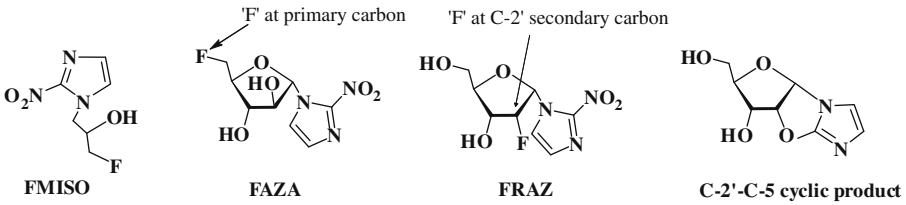

The location of fluorine at a secondary carbon C-2' in FRAZ will minimize possible intramolecular side reactions e.g. the formation of C-2'-C-5' cyclic product[47] as shown here.

Figure 1. Structures of FMISO, FAZA, FRAZ and C-2′-C-5 cyclic product.

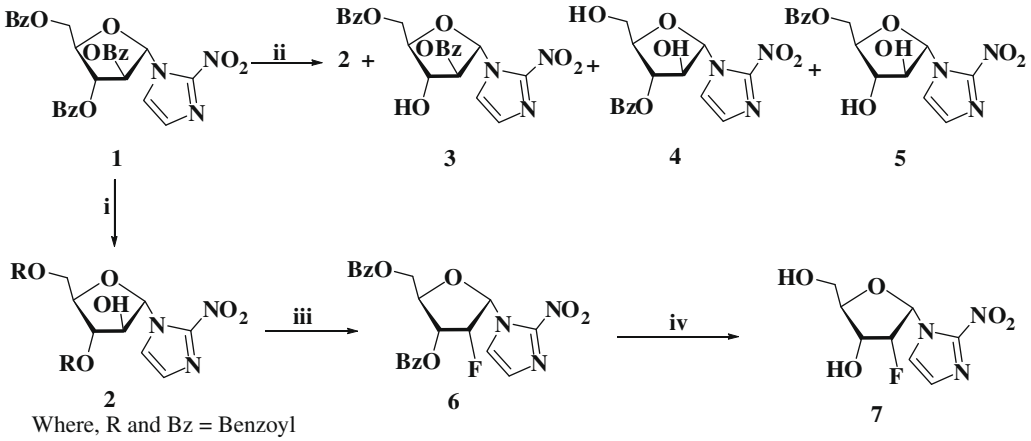

Scheme 1. Synthetic route to FRAZ, **7**. Reagents and conditions: (i) *tert*-BuOK (1 equiv)/THF, −78 °C; (ii) *tert*-BuOK (3 equiv)/THF, −56 °C; (iii) DAST (5 equiv)/CH_2Cl_2/pyridine (4:1, v/v)/ 4 h at 0 °C then 14 h at 22 °C; (iv) 2 M NH_3/MeOH, 0–15 °C, 15 h.

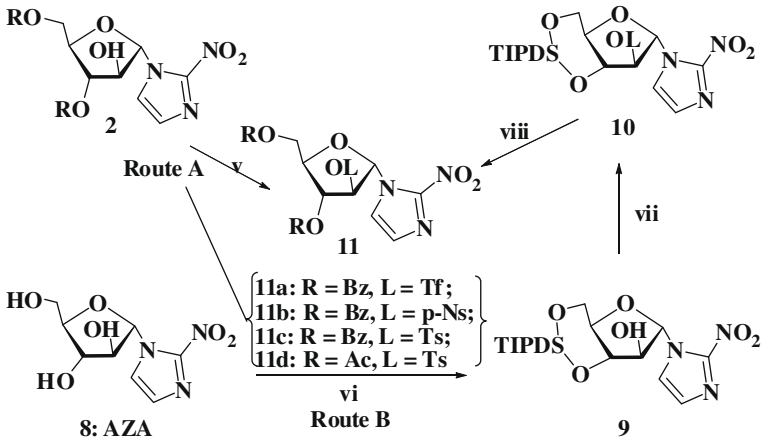

Scheme 2. Synthetic route to the precursors, **11a**–**11d**, for preparing [^{18}F]-**7**. Reagents and conditions: (v) For **11a**, triflyl anhydride/DMAP/anhyd CH_2Cl_2/0 (1 h)→22 °C (3 h); for **11b**, nosyl chloride/AgOTf/0 (1 h)→22 °C (3 h); for **11c**, tosyl chloride/DMAP/anhyd pyridine/45–50 °C (16 h); (vi) TIPDS-Cl/anhyd pyridine/22 °C (16 h); (vii) tosyl chloride/DMAP/anhyd pyridine/22 °C (24 h); (viii) TBAF (THF)/Ac_2O/acetonitrile/22 °C (20 h).

Compound **2** was the main synthon for synthesizing **7** and the precursors that would be used to develop [^{18}F]-**7**). 1-α-D-(3,5-Di-*O*-benzoyl-2-deoxy-2-fluororibofuranosyl)-2-nitroimidazole, **6**, was obtained in excellent yield (>72% isolated yield) by fluorinating **2** with diethylaminosulfurtrifluoride (DAST) under anhydrous conditions. Strong downfield movement in the chemical shifts for H-2′ (by δ 1.08 ppm), H-3′ (by δ 0.15 ppm), H-1′ (by δ 0.32 ppm) protons, and the split in these resonances were attributed to their coupling with fluorine (J_{F-H}) which confirmed the incorporation of fluorine at C-2′ in **6** (Table 1).

The incorporation of fluorine at C-2′ in **6** impacted the NMR signals of H-1′, H-2′, and H-3′ (neighboring protons), as evident by the appearance of a doublet of doublet (dd) at δ 6.94 (H-1′; $J_{F,H1'}$ = 12 Hz), a doublet of doublet of doublet (ddd) at δ 5.77 (H-2′; $J_{F,H2'}$ = 54 Hz) and a ddd at δ 5.64 for (H-3′; $J_{F,H3'}$ = 18 Hz) in its ^{1}H NMR spectrum. ^{19}F NMR and ^{13}C NMR spectroscopic data pro-

Table 1
^{1}H, ^{19}F and ^{13}C NMR chemical shifts and the coupling constants (*J*) of specific compounds **2**–**11** and related coupling constants

Compounds	Chemical shifts (δ ppm) and the splitting patterns (*in italic*)									Coupling constant '*J*' (Hz)		
	H-1′	H-2′	H-3′	H-4′	^{19}F	C-1′	C-2′	C-3′	C-4′	$J_{F,1'}$	$J_{F,2'}$	$J_{F,3'}$
2	6.62 *s*	4.69 *s*	5.49 *s*	5.03 *dd*		96.51	79.05	86.23	82.07			
3	5.34 *s*	5.34 *s*	4.58 *s*	4.90 *dd*		94.65	89.88	81.32	80.11			
6	6.94 *dd*	5.77 *ddd*	5.64 *ddd*	4.99 *dd*	−47.85 *ddd*	88.43 *d* $J_{F,C}$ = 17	88.04 *d* $J_{F,C}$ = 202	71.60 *d* $J_{F,C}$ = 15	79.83	12	54	18
7	6.77 *dd*	5.34 *ddd*	4.70	4.34 *dd*	−46.65 *ddd*	90.11 *d* $J_{F,C}$ = 15	91.94 *d* $J_{F,C}$ = 195	71.17 *d* $J_{F,C}$ = 18	86.01	13	54	20
11b	6.58 *s*	5.44 *s*	5.11 *d*	4.65 *ddd*		92.91	84.75	80.82	76.21			
11c	6.74 *s*	5.70 *s*	5.34 *d*	4.94 *dt*		92.53	85.88	85.88	76.67			
11d	6.58 *s*	5.40 *s*	5.04 *s*	4.69 *ddd*		92.53	85.50	85.50	76.32			

vided additional support to the site-specific fluorination at C-2′ in **6**. The ^{19}F NMR spectrum included a ddd signal at δ −47.85 ($J_{F,2'}$ = 54 Hz, $J_{F,1'}$ = 12 Hz, and $J_{F,H3'}$ = 18 Hz) while ^{13}C NMR spectrum revealed a strong downfield shift of the signal for C-2′ (by δ 8.99 ppm) in comparison to the corresponding non-fluorinated compound **2,** and exhibited fluorine-specific interaction ($J_{F,C2'}$ = 202 Hz). The incorporation of fluorine also created a shielding effect on neighboring carbons, which was reflected by the signals for C-1′ (δ 88.43 ppm, $J_{F,C1'}$ = 17 ppm) and C-3′ (δ 71.60 ppm, $J_{F,C1'}$ = 15 ppm) in the ^{13}C NMR spectrum of **6** (Table 1). The conversion of **6** into **7** was facilitated by NH_3/MeOH-assisted debenzoylation, which proceeded smoothly (74% yield). Removal of benzoyl groups shielded H-1′ and H-2′ in **7** (chemical shifts moved upfield by δ 0.17 ppm and 0.45 ppm, respectively) in comparison to the corresponding dibenzoyl product **6**. In addition, ^{19}F and ^{13}C NMR spectra also demonstrated relevant impact on the carbon chemical shifts (C-1′, C-2′, and C-3′) and exhibited typical fluorine–carbon (F–C) coupling patterns reconfirming the presence of fluorine in the structure of **7** as shown by the relevant chemical shifts and corresponding coupling constants in Table 1.

F-18 radionuclide is short-lived ($t_{1/2}$ = ~110 min), so its facile incorporation requires both an easily substitutable leaving group and easily hydrolyzed protective groups in the precursor molecule to minimize total reaction time. Scheme 2 depicts the syntheses of four precursors that possess these features. They were prepared via two synthetic routes, A and B. Route A followed simple substitution of C-2′-OH group in **2** with an appropriately substituted alkyl/aryl sulfonylchloride.

Thus, the syntheses of 1-α-D-(3,5-di-*O*-benzoyl-2-*O*-triflyl-arabinofuranosyl)-2-nitroimidazole, **11a**, and 1-α-D-(3,5-di-*O*-benzoyl-2′-*O*-tosyl-arabinofuranosyl)-2-nitroimidazole, **11c**, were catalyzed by dimethylaminopyridine (DMAP), while silver triflate was used to promote the reaction of nosyl chloride with **2**. The chemical yields of these derivatives were satisfactory, ranging from 62% to 82%. Compound **11a**, the triflyl analogue, was not very stable even under cold storage conditions. It is reported that the removal of benzoyl groups takes longer and requires stronger alkali which, in the case of azomycin nucleosides, results in the formation of secondary products.[53] Therefore, compound **11d**, an acetyl substituted analogue of **11c**, was also synthesized following route B. This route followed the protection of 3′- and 5′-OH groups in AZA, **8**, with the tetraisopropyldisilanyloxy (TIPDS) group to afford 1-α-D-(3,5-*O*,*O*-TIPDS-arabinofuranosyl)-2-nitroimidazole, **9**[54] in 86% yield. Compound **9**, on reaction with tosyl chloride in the presence of DMAP, gave 1-α-D-(3,5-*O*,*O*-TIPDS-2′-*O*-tosylarabinofuranosyl)-2-nitroimidazole, **10**. ^1H and ^{13}C NMR spectra of **10** confirmed the incorporation of tosyl group at C-2′ OH group. Acetylation of **10** replaced the TIPDS group from 3′-O and 5′-O positions to provide the corresponding 3′,5′-di-*O*-acetyl product **11d** in high yield.

2.2. ^{18}F-labeling

The radiofluorination chemistry of [^{18}F]-FRAZ was based on the nucleophilic substitution of its tosylate precursor, and was performed as shown below (Scheme 3). The –OH groups at the C-5′ and C-3′ positions in the tosylate precursors were protected by the base labile protective groups (acetyl/benzoyl) to render selective fluorination at the C-2′ position possible, to ensure facile post-fluorination deprotection. An automated radiofluorination process for [^{18}F]-**7** at 110 °C (5 min labeling time) using a commercially available automated synthesis unit (ASU), Tracerlab-FX (GE, USA) provided complete synthesis in ~32 min.

The incorporation of F-18, due to its short half-life, requires optimal labeling conditions to avoid unnecessary losses. It has been reported that the base-catalyzed radiofluorination of azomycin nucleoside-based precursors containing vicinal –OH groups competes with the formation of several secondary fluorinated and non-fluorinated products (due to the intramolecular elimination).[47] The leaving groups that create a stronger polarization of 'C-sulfonate' bond, for example, nosylate or triflate[55] may also promote the rate of formation of undesired side products even though they undergo higher rates of substitution. Nucleophilic substitution of the tosyl group is slow relative to triflyl or nosyl groups, and this may translate into lower radiofluorination yields, however, the slower reaction kinetics may also reduce decomposition and/or side product formation during the labeling process. The F-18 labeling of **7** was attempted from its tosylated precursor **11d**. HPLC analysis of the labeled reaction mixture revealed the formation of [^{18}F]-**7** along with unreacted fluoride and several unidentified labeled species which were not isolated (Fig. 2A and B). Purified [^{18}F]-**7** (195 MBq) was collected after HPLC in ~22% radiochemical yield (uncorrected yield; specific activity = 63 GBq/nmol); TLC co-spotting with standard FRAZ indicated a radiochemical purity (Fig. 2C) >97% using a AR 2000 radio-scanner (Bioscan Inc., USA) and UV visualization of standard FRAZ (UV at 254–400 nm; $R_{f[^{18}F]\text{-FRAZ}}$ = ±0.05 $R_{fSTD.\ UV}$).

Chemical stability is essential for in vivo and in vitro evaluations (e.g., PET imaging and radiosensitization measurements). It is well known that halogens substituted on a primary carbon are relatively unstable chemically in comparison to the halogens substituted at a secondary carbon. In the case of IAZA, which has an iodine at the primary C-5′ position, and FMISO, which has fluorine on a primary carbon, in vivo deiodination[48] and metabolic degradation,[56] respectively, occur. On the other hand, [^{18}F]-FAZA, a fluorinated analogue of IAZA, is stable over a 24 h storage period when formulated in 8% ethanol solution in sterile water.[57] Although there is no literature report available on its in vivo stability, other fluorinated nucleosides have been reported to be stable.[49] The reason for the stability of the C–F bond (length 1.35 Å) relative to the C–H bond (length 1.43 Å) may be due to stabilization of the 'endo' conformation in a two carbon unit bonded vicinally to electronegative elements as in 2-deoxy-2-fluoro ribonucleosides.[49,50] It has been proposed that this effect results from the high electronegativity of the fluorine atom acting in conjunction with the '*gauche* effect'.[58] The placement of fluorine at C-2′ position in **7** therefore may provide it a superior in vivo stability in comparison to non-fluorinated azomycin nucleosides.

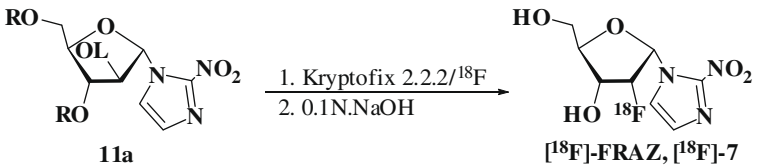

11a **[^{18}F]-FRAZ, [^{18}F]-7**

Scheme 3. Radiofluorination process to synthesize [^{18}F]-**7**.

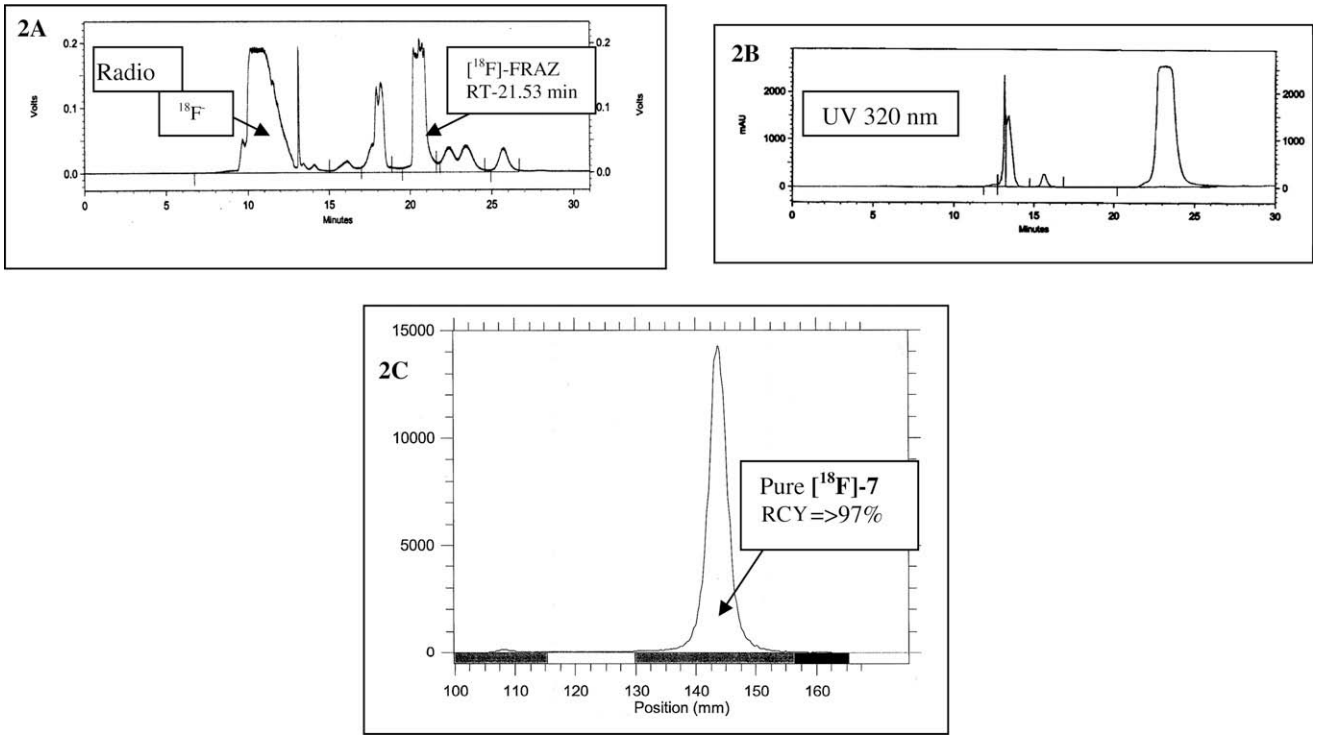

Figure 2. Radio (**2A**) and UV (**2B**; 320 nm) HPLC chromatograms of post-labeling reaction mixture of [^{18}F]-7 from its tosylate precursor, and TLC chromatogram of purified [^{18}F]-7 (**2C**). [^{18}F]-FRAZ is seen at a retention time of 21 min in the radiochromatogram (**2A**). A major peak in the UV chromatogram (**2B**) at a retention time of 23.5 min relates to the formation of an unknown side product.

3. Biological assessment

3.1. Cytotoxicity

FRAZ was evaluated for its cytotoxic effects in vitro in EMT-6 (murine mammary tumor), KBALB, KBALB-STK (Kirsten virus-transformed murine sarcoma cell lines), 143B (human osteosarcoma), and 143B-LTK (human leukemia) cancer cell lines at the concentrations ranging from 10^{-7} to 10^{-3} M (Fig. 3). These data indicated that **7** has only low toxicity in these cell lines at concentrations below 10^{-4} M, and that all cells except the EMT-6 line showed marked reductions in survival at mM (10^{-3} M) concentrations.

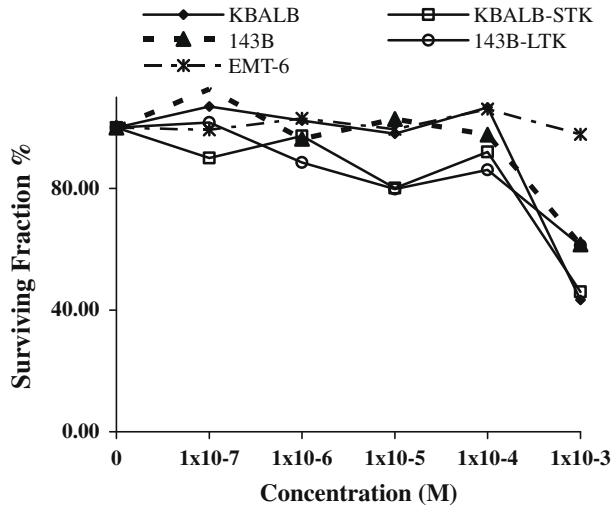

Figure 3. In vitro cytotoxicity of FRAZ, **7**, in KBALB, KBALB-STK, 143B, 143B-LTK and EMT-6 cancer cell lines as assessed by MTT assay.

3.2. Radiosensitization

These studies with **7** were performed in HCT-116 colorectal carcinoma cells (Fig. 4, top frame) at a concentration of 100 μM and were compared with standard hypoxia radiosensitizer FAZA (Fig. 4, lower frame). The toxicity to normoxic cells at this concentration is expected to be minimal. The data showed that the radiosensitization by FRAZ, **7**, at 100 μM concentration is comparable to FAZA, since its oxygen enhancement ratio was ~2.0, although **7** demonstrated a slightly superior sensitization enhancement ratio (SER_{FRAZ} ~1.4 vs. SER_{FAZA} ~1.25) for HCT-116 cancer cell lines. This indicates that the sensitizer enhancement ratio of **7** falls within the range of 1.20–2.14 at 1 mM, and is therefore a potentially useful nitroimidazole-based hypoxia radiosensitizer.[36]

3.3. Partition coefficient (*P*)

The retention times of FRAZ, FAZA and selected α-azomycin nucleosides were compared on reverse phase HPLC. It was observed that the retention times for FRAZ and FAZA were almost identical. Interpolation from a plot of partition coefficients (*P*) of known azomycin nucleosides as a function of their retention times showed that FRAZ is essentially equi-lipophilic (*P* = 1.08) to FAZA (*P* = 1.10).[38] The positional difference in fluorine placements (C-5′ in FAZA and C-2′ in FRAZ), as expected, resulted in very little variation in the lipophilicity (Fig. 5). This falls within the range (*P* = 0.1–10) of log partition coefficients thought to be compatible with good tissue penetration by diffusion.[18,59]

4. Conclusion

The synthesis of FRAZ, **7**, a positional ribose analogue of FAZA, was achieved by DAST-assisted fluorination of **2** in ~74% yield. Preliminary in vitro radiosensitization studies with **7** against HCT-

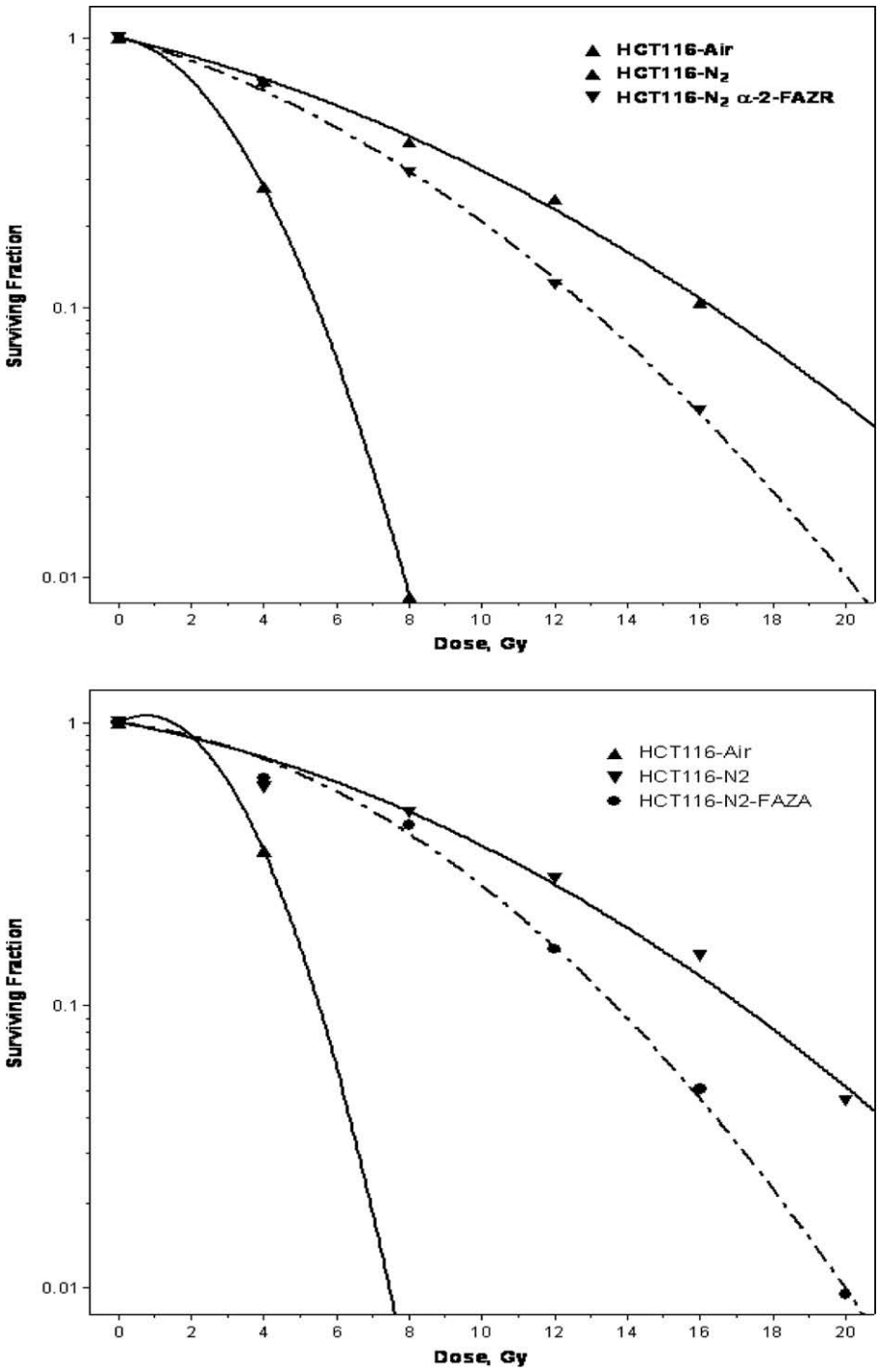

Figure 4. In vitro radiosensitization of HCT-116 colorectal cancer cells (top) by **7** (indicated as α-2-FAZR in the top frame; 100 μM), and by FAZA (100 μM) (bottom), as demonstrated by their survival curves.

116/100 colorectal carcinoma cells indicated that **7** is equipotent to FAZA as a radiosensitizer. The toxicity of FRAZ to oxygenated cells was low, with minimal effect on cell survival at concentrations less that 10^{-3} M. The precursors required for the radiochemical development of [^{18}F]-**7** were based on simple, readily removable protecting groups and leaving groups. Initial F-18 labeling experiments afforded [^{18}F]-**7** in ~22% radiochemical yield (decay uncorrected). FRAZ, **7**, may be more stable in vivo than FAZA due to the influence of fluorine substitution at C-2′ (in comparison to C-5′ in FAZA). It is expected that this positional isomer will possess similar hypoxia-selective accumulation in hypoxic tumors as FAZA since the placement of fluorine at a C-2′ (in comparison to C-5′ in FAZA) in the sugar moiety does not impact its lipophilicity, and therefore, its diffusion properties. It is known that the clinical usefulness of the radiosensitizers with substantially lower partition coefficients is greatly enhanced due to their faster pharmacokinetic renal clearance, as in the case of FAZA,[44] in comparison to more lipophilic compounds like MISO and FMISO that have poor egression resulting in undesirable neurotoxicities[60,61] and slower hepatobiliary clearance.[44] PET imaging and hypoxia-selective in vivo biodistribution and pharmacokinetic studies of FRAZ are warranted.

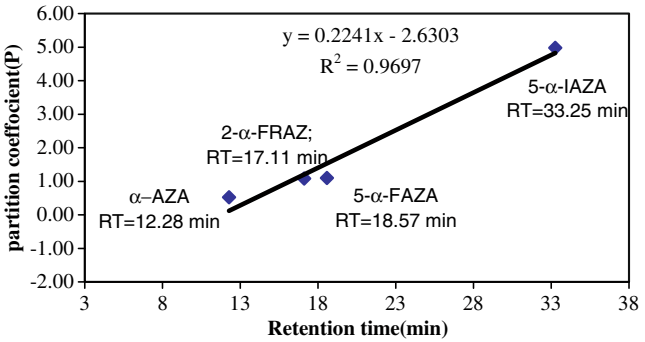

Figure 5. Correlation between partition coefficient (*P* values) and reverse phase HPLC retention times for FRAZ, FAZA and selected α-azomycin nucleosides. The linear regression line was drawn using Microsoft Excel™.

5. Experimental

5.1. General

All chemicals used were of reagent grade. Solvents were dried over appropriate drying agents and freshly distilled before use. The progress of synthetic reactions was monitored by thin layer chromatography (TLC) in a suitable solvent system (system A—5:95, v/v, CH_3OH/CH_2Cl_2; system B—10:90, v/v, CH_3OH/CH_2Cl_2; system C—hexanes/EtOAc, 2:1, v/v; system D—hexanes/EtOAc, 1:2, v/v; and system E—hexanes/EtOAc 1:1, v/v). Column chromatography was performed on Merck Silica Gel 60 (70–200 and 230–400 mesh ASTM). Melting points were determined on a Büchi capillary melting point apparatus and are uncorrected. ^1H, ^{19}F, and ^{13}C NMR spectra were recorded on a Bruker AM-300 spectrometer in deuterated chloroform ($CDCl_3$), dimethylsulfoxide (DMSO-d_6) or methanol (CD_3OD), depending on the solubility of the product. Chemical shifts are reported in δ ppm downfield with respect to tetramethylsilane as an internal standard in ^1H and ^{13}C NMR spectra, and trifluoroacetic acid as an external standard for ^{19}F NMR spectra. The protons and carbons of the sugar moiety and nitroimidazole are represented by a single prime (′) and no prime, respectively. HRMS were recorded using an AEI-MS-12 mass spectrometer. High performance liquid chromatography (HPLC) of ^{18}F-labeled FRAZ was performed on a Beckman HPLC system equipped with an isocratic solvent single flow pump, a reverse phase C-18 guard column (Phenomenex 50 × 10 mm) and column (Phenomenex 250 × 9 mm), dual detectors (UV and radioactive), and Gold software to analyze and quantify the eluted components. The purification was performed using EtOH/sterile H_2O (12:88; v/v) as an eluent at a flow rate of 1.8 mL/min.

5.2. Chemistry

5.2.1. 1-α-D-(2,3,5-Tri-*O*-benzoylarabinofuranosyl)-2-nitroimidazole (1)

Benzoyl chloride (2.30 g, 16.32 mmol) was added drop-wise to a stirred solution of **8** (1 g, 4.08 mmol) in dry pyridine (16 mL) at 0 °C (ice/water bath). The reaction mixture was stirred at 0 °C for 2 h and at 22 °C for 20 h under argon. At this time, the solvent was removed under vacuum (rotary evaporator and water pump) and co-evaporated with toluene (2 × 5 mL). Purification of the residue via flash column chromatography on silica gel using hexanes/EtOAc (2:1→1:1, v/v) as eluent afforded a light yellowish oil, which was crystallized from EtOAc/hexanes (2:1, v/v, 15 mL) to yield **1** (2.26 g, 100%) as white crystals; mp 105–106 °C (observed); 106 °C (reported); R_f 0.68 (system E).[51]

5.2.2. 1-α-D-(3,5-Di-*O*-benzoylarabinofuranosyl)-2-nitroimidazole (2)

tert-BuOK (1.8 mL of 1 M solution in THF, 1.8 mmol, 1 equiv) was added to a solution of **1** (1 g, 1.8 mmol) in THF (15 mL), pre-chilled at −78 °C (dry-ice/acetone bath), with vigorous stirring under an inert (argon) atmosphere. After stirring for 30 min, another portion of 1 M solution of *tert*-BuOK in THF (0.45 mL, 0.45 mmol) was added to the reaction mixture and the resulting solution was stirred for an additional 10 min. A TLC check (solvent system A) at this time indicated complete disappearance of the starting material **2**. The reaction was quenched by the addition of Dowex-50 W resin that neutralized the base (by monitoring with colorpHast™ Indicator strips; pH 0–14). The resin was filtered off, further washed with CH_2Cl_2 (30 mL) and CH_3OH (10 mL) and then the filtrate and the washings were combined to evaporate the solvents under reduced pressure. The residue was purified via flash silica gel column chromatography using hexanes/EtOAc (2:1→1:1, v/v) as eluent to give **2** (0.66 g, 81%) as a white solid; mp 70–71 °C; R_f 0.44 (solvent system A); ^1H NMR ($CDCl_3$): δ 4.69 (s, 1H, H-2′), 4.74 (dd, $J_{4',5'}$ = 6 Hz, J_{gem} = 12 Hz, 1H, H-5′), 4.82 (dd, $J_{4',5''}$ = 7 Hz, J_{gem} = 12 Hz, 1H, H-5″), 5.03 (dd, $J_{5'4'}$ = 6 Hz, $J_{5'',4'}$ = 7 Hz, 1H, H-4′), 5.49 (s, 1H, H-3′), 6.62 (s, 1H, H-1′), 7.22 (s, 1H, H-4), 7.39 (s, 1H, H-5), 7.34–8.14 (m, 10H, two phenyls); ^{13}C NMR ($CDCl_3$): δ 63.94 (C-5′), 79.05 (C-2′), 82.07 (C-4′), 86.23 (C-3′), 96.51 (C-1′), 129.46–130.10 (phenyl carbons), 133.30 (imidazole C-4), 133.87 (imidazole C-5), 143.77 (C-2, imidazole), 165.13 and 166.25 (2 C═O); HRMS for $C_{22}H_{19}N_3O_8Na$, Calcd: 453.07514. Found: 453.07519 (M^+Na, 100%).

5.2.3. 1-α-D-(2,5-Di-*O*-benzoylarabinofuranosyl)-2-nitroimidazole (3)

This product was formed during the synthesis of **2**, and was isolated as a white solid (0.16 g, 20%) during the chromatographic purification of the debenzoylation reaction mixture. Mp 69–70 °C; R_f 0.48 (solvent system A); ^1H NMR (DMSO-d_6 + CD_3OD): δ 3.89 (dd, $J_{4',5'}$ = 6 Hz, J_{gem} = 12 Hz, 1H, H-5′), 3.94 (dd, $J_{4',5''}$ = 5 Hz, J_{gem} = 12 Hz, 1H, H-5″), 4.58 (s, 1H, H-2′), 4.90 (dd, $J_{5'4'}$ = 6 Hz, $J_{5'',4'}$ = 5 Hz, 1H, H-4′), 5.34 (s, 1H, H-3′), 6.56 (s, 1H, H-1′), 7.24 (s, 1H, H-4), 7.43–7.74 (5H, phenyl), 7.85 (s, 1H, H-5); ^{13}C NMR (DMSO-d_6 + CD_3OD): δ 62.85 (C-5′), 80.11 (C-4′), 81.32 (C-2′), 89.88 (C-3′), 94.65 (C-1′), 124.79 (imidazole C-4), 129.24–134.35 (phenyl carbons), 128.30 (imidazole C-5), 144.92 (C-2, imidazole), 166.89 (C═O); HRMS for $C_{22}H_{19}N_3O_8Na$, Calcd: 453.07514. Found: 453.07521 (M^+Na, 100%).

5.2.4. 1-α-D-(3-*O*-Benzoylarabinofuranosyl)-2-nitroimidazole (4) and 1-α-D-(5-*O*-benzoylarabinofuranosyl)-2-nitroimidazole (5)

These compounds were formed when the synthesis of **2** from **1** was attempted at a higher temperature (−56 °C), and using three chemical equivalents of *tert*-BuOK solution (1 M in anhydrous THF). The reaction was complete in 5 min, and afforded **4** as a major product along with small quantities of **2** (~3%), **3** (5%), and **5** (35%). Flash column chromatography of the impure mixture using gradients of hexanes/EtOAc (1:1→1:2→1:3; v/v; 200 mL of each composition) separated these products and gave pure **4** as a solid. Recrystallization from hexanes/EtOAc (3:1; v/v; 6 mL) afforded **4** as white crystals, and **5** as a white solid. The chemical data for these compounds are given below.

Compound **4**: Yield 300 mg (42%); Mp 194–196 °C; R_f 0.34 (solvent system A); ^1H NMR (CD_3OD + DMSO-d_6): δ 3.91 (dd, $J_{4',5'}$ = 5 Hz, J_{gem} = 12 Hz, 1H, H-5′), 3.94 (dd, $J_{4',5''}$ = 6 Hz, J_{gem} = 12 Hz, 1H, H-5″), 4.58 (s, 1H, H-2′), 4.90 (dd, $J_{5'4'}$ = 5 Hz, $J_{5'',4'}$ = 6 Hz, 1H, H-4′), 5.34 (s, 1H, H-3′), 6.56 (s, 1H, H-1′), 7.24 (s, 1H, H-4), 7.43–7.75 (m, 5H, phenyl), 7.85 (s, 1H, H-5); ^{13}C NMR ($CDCl_3$): δ 62.85 (C-5′), 80.11 (C-4′), 81.33 (C-2′), 89.88 (C-3′),

97.42 (C-1′), 129.03 and 130.12 (phenyl carbons), 130.26 (imidazole C-4), 134.35 (imidazole C-5), 144.92 (C-2, imidazole), 165.89 (C=O); HRMS (EI^+) for $C_{15}H_{15}N_3O_7Na$, Calcd: 352.0754. Found: 352.0752 (M^+Na, 100%).

Compound **5**: Yield 250 mg; Mp 198–199 °C; R_f 0.29 (solvent system A); ^1H NMR ($CDCl_3$): δ 4.05 (d, $J_{2',3'}$ = 3 Hz, 1H, H-3′), 4.31 (d, $J_{3',2'}$ = 3 Hz, 1H, H-2′), 4.55 (d, $J_{4',5'}$ = 4 Hz, J_{gem} = 12 Hz, 1H, H-5′), 4.84 (dd, $J_{4',5''}$ = 3 Hz, J_{gem} = 12 Hz, 1H, H-5″), 4.83 (dd, $J_{5'4'}$ = 4 Hz, $J_{5'',4'}$ = 3 Hz, 1H, H-4′), 6.87 (s, 1H, H-1′), 7.19 (s, 1H, H-4), 7.48 (s, 1H, H-5), 7.49–8.05 (m, 5H, phenyl); HRMS (EI^+) for $C_{15}H_{15}N_3O_7Na$, Calcd: 352.0754. Found: 352.0749 (M^+Na, 100%).

5.2.5. 1-α-D-(3,5-Di-*O*-benzoyl-2-deoxy-2-fluororibofuranosyl)-2-nitroimidazole (6)

Compound **2** (0.60 g, 1.32 mmol) was dissolved in CH_2Cl_2/pyridine (10 mL, 98:2, v/v). The solution was cooled to 0 °C, diethylaminosulfurtrifluoride (DAST, 1.06 g, 6.6 mmol) was added, and the mixture was stirred for 4 h at 0 °C, and then for 14 h at 22 °C, under argon. Once the starting material was completely exhausted (TLC), the reaction progress was quenched by adding a small quantity of methanol (5 mL). The solvents were removed under vacuum by toluene co-evaporation (2 × 5 mL) under reduced pressure and the residue was purified by flash silica gel column chromatography using hexanes/EtOAc (1:1, v/v) as eluent which gave **6** (0.435 g, >72%) as a white foam. Mp 56–57 °C; R_f 0.59 (solvent system E); ^1H NMR ($CDCl_3$): δ 4.58 (dd, $J_{4',5'}$ = 4 Hz, J_{gem} = 13 Hz, 1H, H-5′), 4.63 (dd, $J_{4',5''}$ = 3 Hz, J_{gem} = 13 Hz, 1H, H-5″), 4.99 (dd, $J_{3'4'}$ = 4 Hz, $J_{5',4'}$ = 3 Hz, 1H, H-4′), 5.64 (ddd, $J_{2',3'}$ = 4 Hz, $J_{4',3'}$ = 4 Hz, $J_{F,3'}$ = 18 Hz, 1H, H-3′), 5.77 (ddd, $J_{1',2'}$ = 4 Hz, $J_{3',2'}$ = 4 Hz, $J_{F,2'}$ = 54 Hz, 1H, H-2′), 6.94 (dd, $J_{2',1'}$ = 4 Hz, $J_{F,1'}$ = 13 Hz, 1H, H-1′), 7.26 (s, 1H, H-4), 7.41 (s, 1H, H-5), 7.44–8.05 (m, 10H, two phenyls); ^{13}C NMR ($CDCl_3$): δ 62.98 (C-5′), 71.60 (d, $J_{F,4'}$ = 15 Hz, C-3′), 79.83 (C-4′), 88.04 (d, $J_{F,2'}$ = 202 Hz, C-2′), 88.43 (d, $J_{F,1'}$ = 17 Hz, C-2′), 128.06–129.85 (phenyl carbons), 133.55 (imidazole C-4), 133.94 (imidazole C-5), 145.00 (C-2, imidazole), 165.1 and 165.8 (2 C=O); ^{19}F NMR (CD_3OD): δ −47.85 (ddd, $J_{F,1'}$ = 12 Hz, $J_{F,3'}$ = 18 Hz, $J_{F,2'}$ = 54 Hz); HRMS (EI^+) for $C_{22}H_{18}N_3O_7FNa$, Calcd: 478.10210. Found: 478.10231.

5.2.6. 1-α-D-(2-Deoxy-2-fluororibofuranosyl)-2-nitroimidazole (7, FRAZ)

Compound **6** (0.050 g, 0.11 mmol) was treated with a solution of NH_3 in CH_3OH (4 mL of 2 M solution) at 0 °C under argon and the resulting solution was stirred at this temperature for 4 h, and then for 12 h at 22 °C. Once the reaction was complete, the solvent was removed under vacuum and the residue was purified by flash column chromatography on silica gel using 10% CH_3OH in CH_2Cl_2 that gave a white solid. Recrystallization of this material from EtOAc/hexanes (1:1, v/v, 5 mL) yielded **7** (20 mg, 74%) as white crystals. Mp 155–157 °C; R_f 0.46 (system B); ^1H NMR (CD_3OD): δ 3.71 (dd, $J_{4',5'}$ = 3 Hz, J_{gem} = 13 Hz, 1H, H-5′), 3.90 (dd, $J_{2',5''}$ = 2 Hz, J_{gem} = 13 Hz, 1H, H-5″), 4.34 (dd, $J_{3'4'}$ = 4 Hz, $J_{5',4'}$ = 3 Hz, 1H, H-4′), 4.70 (ddd, $J_{2',3'}$ = 4 Hz, $J_{4',3'}$ = 4 Hz, $J_{F,3'}$ = 20 Hz, 1H, H-3′), 5.34 (ddd, $J_{1',2'}$ = 4 Hz, $J_{3',2'}$ = 4 Hz, $J_{F,2'}$ = 54 Hz, 1H, H-2′), 6.77 (dd, $J_{2',1'}$ = 4 Hz, $J_{F,1'}$ = 13 Hz, 1H, H-1′), 7.19 (s, 1H, H-4), 7.72 (s, 1H, H-5); ^{13}C NMR (CD_3OD): δ 61.93 (C-5′), 71.17 (d, $J_{F,3'}$ = 18 Hz, C-3′), 86.01 (C-4′), 90.11 (d, $J_{F,1'}$ = 15 Hz, C-1′), 91.94 (d, $J_{F,2'}$ = 195 Hz, C-2′), 124.97 (imidazole C-4), 128.44 (imidazole C-5), 139.00 (C-2, imidazole); ^{19}F NMR (CD_3OD): δ −46.65 (ddd, $J_{F,1'}$ = 13 Hz, $J_{F,3'}$ = 20 Hz, $J_{F,2'}$ = 54 Hz). Anal. Calcd for $C_8H_{10}FN_3O_5$ (247.18): C, 38.87; H, 4.08; N, 17.00. Found: C, 38.80; H, 4.01; N, 16.89.

The syntheses of the compounds **11a**–**11c** involved the reaction of compound **2** with the appropriate sulfonyl chloride/anhydride following route A, and are described below.

5.2.7. 1-α-D-(3,5-Di-*O*-benzoyl-2-*O*-trifluoromethanesulfonylarabinofuranosyl)-2-nitroimidazole (11a)

Triflyl anhydride (0.0.06 g, 0.35 mmol) was added to a solution of **2** (0.08 g, 0.176 mmol) and DMAP (0.065 g, 0.53 mmol) in anhydrous CH_2Cl_2 (5 mL), and stirred for 2 h at 0 °C under argon. The TLC at this stage showed no change. Another aliquot of triflyl anhydride was added to the reaction mixture, the temperature was then raised to 22 °C, and the stirring was continued for an additional 3 h under argon. The progress of the reaction was quenched by adding a small piece of ice, the solution diluted by adding CH_2Cl_2, and extracted. The organic phase was separated, dried over anhydrous Na_2SO_4, filtered, and the solvent was evaporated under reduced pressure to afford a viscous residue which was purified by flash silica gel column chromatography using hexanes/EtOAc (1:1, v/v) as an eluent to give pure **11a** (0.064 g, 62%) as a colorless viscous oil that was not very stable under normal storage conditions, and could be characterized only by its proton spectrum. R_f 0.6 (system E); ^1H NMR ($CDCl_3$): δ 4.68 (dd, $J_{5',4'}$ = 6 Hz, J_{gem} = 13 Hz, 1H, H-5′), 4.76 (dd, $J_{5'',4'}$ = 6 Hz, J_{gem} = 12 Hz, 1H, H-5″), 5.09 (dd, $J_{5',4'}$ = 5 Hz, $J_{5'',4'}$ = 6 Hz, 1H, H-4′), 5.73 (s, 1H, H-3′), 5.81 (s, 1H, H-2′), 6.96 (s, 1H, H-1′), 7.31 (s, 1H, H-4), 7.39 (s, 1H, H-5), 7.41–8.11 (m, 10H, aromatic).

5.2.8. 1-α-D-(3,5-Di-*O*-benzoyl-2-*O*-(4-nitrobenzenesulfonyl)arabinofuranosyl)-2-nitroimidazole (11b)

Compound **2** (0.15 g, 0.33 mmol) was dissolved in anhydrous pyridine (10 mL) at 0 °C, and nosyl chloride (0.22 g, 0.99 mmol) and silver triflate (AgOTf; 0.255 g, 0.99 mmol) were added to this solution under argon. The reaction mixture was stirred at 0 °C for 1 h and then the temperature was raised to 22 °C. The stirring was continued at this temperature for an additional 3 h, and then the reaction was quenched by adding a small piece of ice. The solvents were evaporated and co-evaporated with toluene (2 × 10 mL) under reduced pressure and the viscous residue was purified by flash silica gel column chromatography using 3% CH_3OH in CH_2Cl_2 as eluent to afford **11b** as a solid. Recrystallization of this material from hexanes/EtOAc (1:1, v/v, 5 mL) produced white crystals of **11b**. Yield 0.20 g (95%); Mp 53–54 °C; R_f 0.6 (system A); ^1H NMR ($CDCl_3$): δ 1.99 and 2.20 (2 s, each for 3H of CH_3), 4.41 (dd, $J_{5',4'}$ = $J_{4',5''}$ = 5 Hz, J_{gem} = 17 Hz, 2H, H-5′ and H-5″), 4.65 (ddd, $J_{3',4'}$ = 3 Hz, $J_{5',4'}$ = 5 Hz, J_{gem} = 17 Hz, 1H, H-4′), 5.11 (d, $J_{4',3'}$ = 3 Hz, 1H, H-3′), 5.44 (s, 1H, H-2′), 6.58 (s, 1H, H-1′), 7.19 (s, 1H, H-4), 7.31 (s, 1H, H-5), 8.15 and 8.43 (2 d, each for 2H of nosylate phenyl); ^{13}C NMR ($CDCl_3$): δ 20.42 and 20.48 (2 CH_3), 68.55 (C-5′), 76.21 (C-4′), 80.82 (C-3′), 84.75 (C-2′), 92.91 (C-1′), 124.52 (two phenyl carbons), 121.77 (imidazole C-4), 128.54 (imidazole C-5), 129.30 (two phenyl carbons), 141.02 (C-4 phenyl), 146.74 (C-2, imidazole), 150.95 (C-1 of phenyl), 168.68 and 169.28 (2 × C=O). Anal. Calcd for $C_{18}H_{18}N_4O_{12}S$ (514.43): C, 52.67; H, 3.47; N, 8.77. Found: C, 52.22; H, 3.14; N, 8.56.

5.2.9. 1-α-D-(3,5-Di-*O*-benzoyl-2-*O*-toluenesulfonylarabinofuranosyl)-2-nitroimidazole (11c)

Compound **2** (0.20 g, 0.44 mmol), tosyl chloride (0.252 g, 1.32 mmol) and DMAP (0.161 g, 1.32 mmol) were dissolved in anhydrous pyridine (15 mL) and stirred at 45–50 °C for 16 h under argon. The TLC examination of the reaction mixture at this time showed no evidence of **2**. The reaction progress was quenched by adding a small piece of ice to this mixture and the solvent was removed under reduced pressure using two co-evaporations with toluene (2 × 20 mL). The viscous residue so obtained was purified by flash silica gel column chromatography. An elution with hexanes/EtOAc (2:1→1:1, v/v, 5 mL) gave pure **11c** (0.22 g, 82%) as a white foam. Mp 60–61 °C; R_f 0.64 (system E); ^1H NMR ($CDCl_3$): δ

2.39 (s, 1H, tosyl CH_3), 4.61 (dd, $J_{5',4'}$ = 6 Hz, J_{gem} = 12 Hz, 1H, H-5′), 4.72 (dd, $J_{5'',4'}$ = 6 Hz, J_{gem} = 12 Hz, 1H, H-5″), 4.94 (dt, $J_{5',4'} = J_{5'',4'}$ = 6 Hz, $J_{3',4'}$ = 2 Hz, 1H, H-4′), 5.34 (d, $J_{4',3'}$ = 2 Hz, 1H, H-3′), 5.70 (s, 1H, H-2′), 6.74 (s, 1H, H-1′), 7.21 (s, 1H, H-4), 7.39 (s, 1H, H-5), 7.30–8.13 (m, 14H, aromatic); ^{13}C NMR ($CDCl_3$): δ 21.72 (CH_3), 63.56 (C-5′), 76.67 (C-4′), 85.88 (C-2′ and C-3′), 92.94 (C-1′), 127.86 (C-4), 128.12–129.73 (phenyl carbons), 131.96 (C-5), 133.37 and 134.09 (tosyl aromatic carbons), 146.21 (C-2, imidazole), 164.47 and 165.91 (2 × C=O). Anal. Calcd for (607.59): C, 57.33; H, 4.15; N, 6.92. Found: C, 57.98; H, 4.07; N, 6.41.

Synthesis of compound **11d** was developed from compound **9** via route B, and is described below.

5.2.10. 1-α-D-(3,5-*O*,*O*-Tetraisopropyldisilanyloxyarabinofuranosyl)-2-nitroimidazole (9)

This product was synthesized following a reported procedure; mp 83–84 °C (observed); 83–84 °C (reported).[54]

5.2.11. 1-α-D-(3,5-*O*,*O*-Tetraisopropyldisilyloxy-2-*O*-toluenesulfonylarabinofuranosyl)-2-nitroimidazole (10)

A mixture of **9**[55] (0.30 g, 0.615 mmol), tosyl chloride (0.35 g, 1.85 mmol), and DMAP (24 mg, 0.02 mmol) were taken in anhydrous pyridine (5 mL) and stirred at 22 °C under an atmosphere of argon for 24 h. At this time, a TLC examination of the reaction mixture showed no change in the status of starting material. Therefore, additional quantities of tosyl chloride (1.85 mmol) and DMAP (0.06 mmol) were added to this reaction mixture and the reaction was subjected to stirring at 60 °C for an additional 21 h that led to the completion of tosylation of **9**. Excess tosyl chloride was hydrolyzed by addition of a small piece of ice, and then the solvents were removed under reduced pressure by evaporation and co-evaporation using toluene (2 × 20 mL). The resulting viscous mass was purified by flash silica gel column chromatography using hexanes/EtOAc (3:1, v/v) as eluent to afford pure solid product, **10**. Recrystallization of this solid from hexanes (20 mL) gave pure white crystals of the product. Yield 340 mg (86%); mp 113–115 °C; R_f 0.5 (solvent system C); ^{1}H NMR ($CDCl_3$): δ 0.98–1.1 (m, 28H, TIPDS protons), 2.44 (s, 1H, tolyl CH_3), 3.91 (dd, $J_{5',4'}$ = 6 Hz, J_{gem} = 12 Hz, 1H, H-5′), 4.03 (dd, $J_{5'',4'}$ = 3 Hz, J_{gem} = 12 Hz, 1H, H-5″), 4.19 (ddd, $J_{5',4'}$ = 6 Hz, $J_{5'',4'}$ = 3 Hz, $J_{3',4'}$ = 5 Hz, 1H, H-4′), 4.67 (dd, $J_{4',3'}$ = 5 Hz, $J_{2',3'}$ = 5 Hz,1H, H-3′), 5.21 (dd, $J_{3',2'}$ = 5 Hz, $J_{1',2'}$ = 4 Hz, 1H, H-2′), 6.55 (d, $J_{1',2'}$ = 4 Hz, 1H, H-1′), 7.18 (s, 1H, H-4), 7.36 (s, 1H, H-5), 7.27–7.65 (2 d, 4H, aromatic); ^{13}C NMR ($CDCl_3$): δ 12.28–17.42 (TIPDS carbons), 21.70 (CH_3), 62.03 (C-5′), 75.75 (C-4′), 85.01 (C-3′), 87.91 (C-2′), 88.82 (C-1′), 122.10 (C-4), 128.66 (C-5), 127.61, 130.01, 131.92 and 146.08 (phenyl carbons) and 144.51 (C-2 imidazole); HRMS (EI$^+$) for $C_{27}H_{43}N_3O_9NaSi_2S$, Calcd: 664.21508. Found: 664.21529.

5.2.12. 1-α-D-(3,5-Di-*O*-acetyl-2-*O*-toluenesulfonylarabinofuranosyl)-2-nitroimidazole (11d)

TBAF (0.94 mL, 1 M solution in anhydrous THF) was added to a solution of **10** (0.30 g, 0.47 mmol) and acetic anhydride (0.38 g, 3.76 mmol) in acetonitrile (6 mL), and the resulting mixture was stirred at 22 °C for 20 h under argon. At this time, TLC of the mixture showed complete disappearance of the silylated precursor and appearance of a new product at a higher R_f. The solvents were removed under reduced pressure, and the dry residue was purified by flash silica gel column chromatography using hexanes/EtOAc (1:2, v/v) to afford pure **11d** as a white foam. Yield 203 mg (90%); mp 50–51 °C; R_f 0.52 (solvent system D); ^{1}H NMR ($CDCl_3$): δ 1.96 and 2.14 (2 s, each for 3H of acetyl CH_3), 2.44 (s, 1H, tosyl CH_3), 4.03 (dd, $J_{5',4'}$ = 6 Hz, J_{gem} = 12 Hz, 1H, H-5′), 4.36 (dd, $J_{5'',4'}$ = 3 Hz, J_{gem} = 12 Hz, 1H, H-5″), 4.69 (ddd, $J_{5',4'}$ = 6 Hz, $J_{5'',4'}$ = 3 Hz, $J_{3',4'}$ = 5 Hz, 1H, H-4′), 5.04 (s,1H, H-3′), 5.40 (s, 1H, H-2′), 6.58 (s, 1H, H-1′), 7.18 (s, 1H, H-4), 7.27 (s, 1H, H-5), 7.38 and 7.83 (2 d, 4H, aromatic); ^{13}C NMR ($CDCl_3$): δ 20.48 and 20.71 (acetyl carbons), 21.79 (tosyl CH_3), 62.86 (C-5′), 76.32 (C-4′), 85.50 (C-2′ and C-3′), 92.53 (C-1′), 122.16 (C-4), 128.18 (C-5), 130.14, 131.77 and 146.26 (phenyl carbons) and 151.16 (C-2 imidazole), 168.83 and 170.40 (2 C=O); HRMS (EI$^+$) for $C_{19}H_{21}N_3O_{10}NaS$, Calcd: 506.08399. Found: 506.08409.

5.3. Radiochemistry

A TR19 negative ion accelerating cyclotron capable of accelerating protons to 19 MeV and deuterons to 9.5 MeV (Advanced Cyclotron Systems, Inc.) with an external high performance multicusp ion source greater than 150 μA beam current with dual simultaneous beam extraction was used for ^{18}F production. A radiofluoride target consisting of a niobium body with HAVAR foil window was used for production of ^{18}F via ^{18}O(p,n)^{18}F reaction by irradiating highly ^{18}O enriched (98%) water ($H_2{}^{18}O$). Tracerlab-FX automated synthesis units (ASU) employed for the manufacture of [^{18}F]-FRAZ was purchased from G.E. Medical Technologies Inc., Canada which operates on the basis of performing unit operations under computer (CPU) control, involving the movement of liquids, movement of gases (vacuum and pressure), valve actuation and heating systems on a time dependent basis through a well defined flow path. Feedback control, monitoring and diagnostic functions are built into the operation using various sensor-based systems.

[^{18}F]Fluoride (1.2 GBq) was transferred to the ASU reaction vessel in a solution containing potassium carbonate (3.5 mg in 100 μL of sterile water for injection, SWFI) and Kryptofix 2.2.2 (15 mg in 900 μL of CH_3CN). The solvents from the fluoride complex were removed by two azeotropic evaporations and then **11a** (5 mg predissolved in 1 mL of anhydrous DMSO) was added to it and heated at 110 °C (5 min). The total reaction time was ~32 min. The resulting product was then deprotected using 0.1 N NaOH (2 min at 30 °C) and the pH was adjusted to ~5–7.5 by adding 0.4 M NaH_2PO_4 buffer (1 mL). HPLC purification of this crude mixture on a C-18 reversed phase column (10 ODS3, 25 × 0.9 cm) using 12% EtOH in SWFI as eluent (flow rate 1.8 mL/min) revealed the presence of [^{18}F]-**7** along with unreacted [^{18}F]-fluoride (10–13 min); pure [^{18}F]-**7** (195 MBq; ~22% radiochemical yield, decay uncorrected, radiochemical purity = >97%) was recovered at a retention time of 21 min (±5%) (specific activity = 63 GBq/nmol). The purity of the HPLC-purified radiopharmaceutical was checked by TLC examination using a BIOSCAN TLC AR2000 scanner and the radiochemical identity was confirmed by comparing its R_f with by co-spotting the standard FRAZ, **7** (Fig. 2C).

5.4. Cytotoxicity

Briefly, exponentially-growing cells were trypsinized and collected in the appropriate medium. The cell concentrations were adjusted to 8×10^3 cells/mL with the corresponding medium. The cells (8×10^2 cells in 100 μL) were seeded into wells of a 96-well plate and incubated for 24 h at 37 °C with 5% CO_2 and 95% air.[62] Compound **7** was dissolved at the desired concentrations in growth medium and the resulting solution (100 μL) of test compound was added to each cell-containing well. In controls, 100 μL of the medium replaced the compound solution. After incubation for 72 h at 37 °C, (3-(4,5-dimethylthiazol-2-yl)-2,5-diphenyl tetrazolium bromide (MTT, 50 μL of 1 mg/mL solution) was added to each well, and after 4 h the supernatant was removed and DMSO (150 μL) was added to each well to dissolve the formazan crystals. The plates were then scanned at 540 nm using an ELISA reader. The results indicating cytotoxicity potential of **7** are shown in Figure 3.

5.5. Radiosensitization

Cell radiosensitization for **7** and FAZA, the standard, was determined using a ^{60}Co X-ray source together with a clonogenic survival assay.[37] Briefly, HCT-116/100 human colorectal carcinoma cells (300,000 cells in 3 mL DMEM/F12 medium per T60 Petri dish) were incubated under 5% CO_2 in air at 37 °C for 20 h, then the test substance (**7** and FAZA; stock solution 10 mM in 95% ethanol) was added to achieve a concentration of 100 μM, and incubation continued for 24 h. The dishes were assigned to either the control (normoxic) or hypoxic groups. Those in the hypoxic group were de-gassed to hypoxia by six consecutive vacuum and nitrogen fill cycles in a vacuum chamber. The Petri dishes (hypoxic and normoxic controls) were incubated for 30 min on an oscillating shaker at R/T × 60 cycles per min and then irradiated in a ^{60}Co γ-irradiator at 0 (control), 4, 8, 12, 16, and 20 Gray (Gy) in N_2 (hypoxic sub-group) and air chambers (normoxic sub-group). The cells were then recovered from each dish by two consecutive washes with phosphate buffer saline (PBS) followed by the addition of trypsin (500 μL) and quenching with fresh medium (4.5 mL). Cells were then plated at densities from 100 to 15,000 cells/5 mL medium for normoxic conditions and 100 and 5000 cells/5 mL medium for hypoxic conditions. The cells were incubated for 10–14 days at 37 °C under 5% CO_2, then stained with methylene blue or crystal violet in ethanol, clones counted and surviving fractions were calculated. Tests were done in triplicate. Data for **7** in HCT-116 cells and EMT-6 cells and FAZA in HCT-116 carcinoma cells, all at 100 μM, are presented in Figure 4.

5.6. Partition coefficients (*P*)

The *P* value for FRAZ was determined by comparing the retention time of FRAZ with those of IAZA, FAZA, and AZA using a gradient solvent system on a reverse phase analytical column (25 × −0.4 cm) HPLC, and interpolating from a plot (Fig. 5) of retention time plotted as a function of 1-octanol/water partition coefficients taken from the literature.[37,63,64]

Acknowledgments

The authors thank Alberta Cancer Research Institute and a Proof-of-Principal grant from Canadian Institutes of Health Research for financial support to this project. Automated equipment support and the ^{18}F-supply from the Edmonton PET Centre are gratefully acknowledged.

References and notes

1. Lu, H.; Forbes, R. A.; Verma, A. *J. Biol. Chem.* **2002**, *277*, 23111.
2. Schafer, M.; Ewald, N.; Schafer, C.; Stapler, A.; Piper, H. M.; Noll, T. *FASEB J.* **2003**, *17*, 449.
3. Carroll, V. A.; Ashcroft, M. *Cancer Res.* **2006**, *66*, 6264.
4. Brahimi-Horn, M. C.; Chiche, J.; Pouysségur, J. *Curr. Opin. Cell Biol.* **2007**, *19*, 1.
5. Nordsmark, M.; Overgaard, M.; Overgaard, J. *Radiother. Oncol.* **1996**, *41*, 31.
6. Nordsmark, M.; Alsner, J.; Keller, J.; Nielsen, O. S.; Jensen, O. M.; Horsman, M. R.; Overgaard, J. *Br. J. Cancer* **2001**, *84*, 1070.
7. Nordsmark, M.; Bentzen, S. M.; Rudat, V.; Brizel, D.; Lartigau, E.; Stadler, P.; Becker, A.; Adam, M.; Molls, M.; Dunst, J.; Terris, D. J.; Overgaard, J. *Radiother. Oncol.* **2005**, *77*, 18.
8. Lee, N. Y.; Le, Q. T. *Semin. Oncol.* **2008**, *35*, 236.
9. Brown, J. M.; Giaccia, A. J. *Cancer Res.* **1998**, *58*, 1408.
10. Hall, E. J. In *Radiobiology for the Radiobiologist*; J.B. Lippincott Co.: Philadelphia, USA, 1994.
11. Krohn, K. A.; Link, J. M.; Mason, R. P. *J. Nucl. Med.* **2008**, *49*, 129S.
12. Postema, E. J.; McEwan, A. J. B.; Riauka, T. A.; Kumar, P.; Richmond, D.; Wiebe, L. I. *European J. Nucl. Med. Mol. Imaging* **2009**, *36*, 1565.
13. Vaupel, P. *Oncologist* **2008**, *13*, 21.
14. Nagasawa, H.; Uto, Y.; Kirk, K. L.; Hori, H. *Biol. Pharm. Bull.* **2006**, *29*, 2335.
15. Palcic, B.; Faddegon, B.; Skarsgard, L. D. *Radiat. Res.* **1984**, *100*, 340.
16. Adams, G. E.; Cooke, M. S. *Int. J. Radial. Biol. Relat. Stud. Phys. Chem. Med.* **1969**, *15*, 457.
17. Biaglow, J. E.; Varnes, M. E.; Roizen-Towle, L.; Clark, E. P.; Epp, E. R.; Astor, M. B.; Hall, E. J. *Biochem. Pharmacol.* **1986**, *35*, 77.
18. Brown, J. M.; Workman, P. *Radiat. Res.* **1980**, *82*, 171.
19. Adams, G. E.; Flockhart, I. R.; Smithen, C. E.; Stratford, I. J.; Wardman, P.; Watts, M. E. *Radiat. Res.* **1976**, *67*, 9.
20. Zhang, L.; Gong, A.; Ji, J.; Wu, Y.; Zhu, X.; Lv, S.; Lv, H.; Sun, X. *BMC Cancer* **2007**, *7*, 188.
21. Koh, W. J.; Rasey, J. S.; Evans, M. L.; Grierson, J. R.; Lewellen, T. K.; Graham, M. M.; Krohn, K. A.; Griffin, T. W. *Int. J. Radiat. Oncol. Biol. Phys.* **1992**, *22*, 199.
22. McNeil, T. H.; Koek, L. L.; Brown, S. A.; Hamill, R. W.; Wu, J. Y. *Int. J. Radiat. Oncol. Biol. Phys.* **1986**, *12*, 1067.
23. Cairns, R. A.; Bennewith, K. L.; Graves, E. E.; Giaccia, A. J.; Chang, D. T.; Denko, N. C. *Clin. Cancer Res.* **2009**, *15*, 7170.
24. Busk, M.; Horsman, M. R.; Jakobsen, S.; Hansen, K. V.; Bussink, J.; Kogel, A. V.-D.; Overgaard, J. *J. Radiother. Oncol.* **2009**, *92*, 429.
25. Koch, C. J.; Evans, S. M. *Adv. Exp. Med. Biol.* **2003**, *510*, 285.
26. Pennacchietti, S.; Michieli, P.; Galluzzo, M.; Mazzone, M.; Giordano, S.; Comoglio, P. M. *Cancer Cell.* **2003**, *3*, 347.
27. Denny, W. A. *Eur. J. Med. Chem.* **2001**, *36*, 577.
28. Weissleder, R.; Mahmood, U. *Radiobiology* **2001**, *219*, 316.
29. Caldwell, J. H.; Revenaugh, J. R.; Martin, G. V.; Johnson, P. M.; Rasey, J. S.; Krohn, K. A. *J. Nucl. Med.* **1995**, *36*, 1633.
30. Piert, M.; Machulla, H.; Becker, G.; Stahlschmidt, A.; Patt, M.; Dibmann, P. D.; Fischer, H.; Becker, H. D.; Lauchart, W. *Eur. J. Nucl. Med.* **1999**, *26*, 95.
31. Bottaro, D. P.; Liotta, L. A. *Nature* **2003**, *423*, 593.
32. Evans, S. M.; Kachur, A. V.; Shiue, C.-Y.; Hustinx, R.; Jenkins, W. T.; Shive, G. G.; Karp, J. S.; Alavi, A.; Lord, E. M.; Dolbier, W. R., Jr.; Koch, C. J. *J. Nucl. Med.* **2000**, *41*, 327.
33. Gronroos, T.; Eskola, O.; Lehtio, K.; Minn, H.; Marjamaki, P.; Bergman, J.; Haaparanta, M.; Forsback, S.; Solin, O. *J. Nucl. Med.* **2001**, *42*, 1397.
34. Kumar, P.; McQuarrie, S. A.; Zhou, A.; McEwan, A. J. B.; Wiebe, L. I. *J. Nucl. Med. Biol.* **2005**, *32*, 647.
35. Kumar, P.; Wiebe, L. I.; Beiki, D.; Ohkura, K.; Seki, K.-I. *Tetrahedron Lett.* **2002**, *43*, 4427.
36. Mannan, R. H. *Radioiodinated Sugar-coupled 2-Nitroimidazoles: Novel non-invasive Markers of Hypoxic Tumor Tissue*. Ph.D. Thesis, University of Alberta, Edmonton, 1991.
37. Kumar, P.; Stypinski, D.; Xia, H.; McEwan, A. J. B.; Machulla, H.-J.; Wiebe, L. I. *J. Labelled Compd. Radiopharm.* **1999**, *42*, 3.
38. Piert, M.; Machulla, H.-J.; Picchio, M.; Reischl, G.; Zeigler, S.; Kumar, P.; Wiebe, L. I.; Schwaiger, M. *J. Nucl. Med.* **2005**, *46*, 106.
39. Reischl, G.; Ehrlichmann, W.; Bieg, C.; Kumar, P.; Wiebe, L. I.; Machulla, H.-J. *Appl. Radiat. Isot.* **2005**, *62*, 897.
40. Beck, R.; Röper, B.; Carlsen, J. M.; Huisman, M. C.; Lebschi, J. A.; Andratschke, N.; Picchio, M.; Souvatzoglou, M.; Machulla, H.-J.; Piert, M. *J. Nucl. Med.* **2007**, *486*, 973.
41. Souvatzoglou, M.; Grosu, A.; Röper, B.; Krause, B.; Beck, R.; Reischl, G.; Picchio, M.; Machulla, H.-J.; Wester, H.-J.; Piert, M. *Eur. J. Nucl. Med. Mol. Imaging* **2007**, *34*, 1566.
42. Reischl, G.; Ehrlichmann, W.; Hammerschmidt, F.; Woschek, A.; Lamparter, D.; Kneilling, M.; Maier, F.; Pichler, B. J.; Machulla, H.-J. *J. Nucl. Med.* **2007**, *48*, 292P.
43. Reichel, G.; Sabbah, A.; Machulla, H-J. *J. Labelled Compd. Radiopharm.* **2007**, *50*, S429.
44. Sorger, D.; Patt, M.; Kumar, P.; Wiebe, L. I.; Barthel, H.; Seese, A.; Dannenberg, C.; Tannapfel, A.; Osama Sabri, R. K. *Nucl. Med. Biol.* **2003**, *30*, 317.
45. http://clinicaltrials.gov/ct/show/NCT00388687. *Prognostic Impact in Cervical Cancer*. Medical University of Vienna, Austria, 2006.
46. clinicaltrials.gov/ct2/show/NCT00756691. Cross Cancer Institute, Edmonton, Canada, 2007.
47. Kumar, P.; Emami, S.; McEwan, A. J. B.; Wiebe, L. I. *Lett. Drug Design* **2009**, *6*, 82.
48. McEwan, A. J. B. et al. Unpublished.
49. Liu, P.; Sharon, A.; Chu, C. K. *J. Fluorine Chem.* **2008**, *129*, 743.
50. Kawasaki, A. M.; Caper, D. M.; Susan, M.; Freier, S. M.; Lesnik, E. A.; Zounes, M. C.; Cummins, L. L.; Carolyn, G. C.; Cook, D. M. *J. Med. Chem.* **1993**, *36*, 831.
51. Kumar, P.; Wiebe, L. I.; Atrazheva, E.; Tandon, M. *Tetrahedron Lett.* **2001**, *42*, 2077.
52. Nishino, S.; Takamura, H.; Ishido, Y. *Tetrahedron* **1986**, *42*, 1995.
53. Kumar, P. et al. Unpublished.
54. Kumar, P.; Emami, S.; McEwan, A. J. B.; Wiebe, L. I. *Bioorg. Med. Chem. Lett.* **2008**, *18*, 3256.
55. Jacobson, O.; Bechor, Y.; Icar, A.; Novac, N.; Birman, A.; Marom, H.; Fedeeva, L.; Golan, E.; Leibovitch, I.; Gutman, M.; Even-Spair, E.; Chisin, R.; Gozin, M.; Mishani, E. *Bioorg. Med. Chem.* **2005**, *13*, 6195.
56. Kwock, L.; Gill, M.; McMurry, H. L.; Beckman, W.; Raleigh, J. A.; Joseph, A. P. *Radiat. Res.* **1992**, *129*, 7.
57. Clinical Trial Application. [^{18}F]-FAZA Module 3. Cross Cancer Institute, Edmonton, 2005.
58. Braasch, D. A.; Jensen, S.; Liu, Y.; Kaur, K.; Arar, K.; White, M. A.; Corey, D. R. *Biochemistry* **2003**, *42*, 7967.
59. Van der Kelen, G. P.; Eeckhaut, Z. *J. Mol. Spectrosc.* **1963**, *10*, 141.
60. Brown, J. M.; Lemmon, M. J. *Radiat. Oncol.* **1991**, *20*, 151.
61. Stypinski, D. Ph.D. Thesis, University of Alberta, Edmonton, Alberta, Canada, 1997.
62. Jette, D. C.; Wiebe, L. I.; Flanagan, R. J.; Lee, J.; Chapman, J. D. *Radiat. Res.* **1986**, *105*, 169.
63. Biskupiak, J. E.; Grierson, J. R.; Rasey, J. S.; Martin, G. V.; Krohn, K. A. *J. Med. Chem.* **1991**, *34*, 2165.
64. Kumar, P.; Emami, S.; Kresolek, Z.; Yang, J.; McEwan, A. J. B.; Wiebe, L. I. *Med. Chem.* **2009**, *5*, 118.